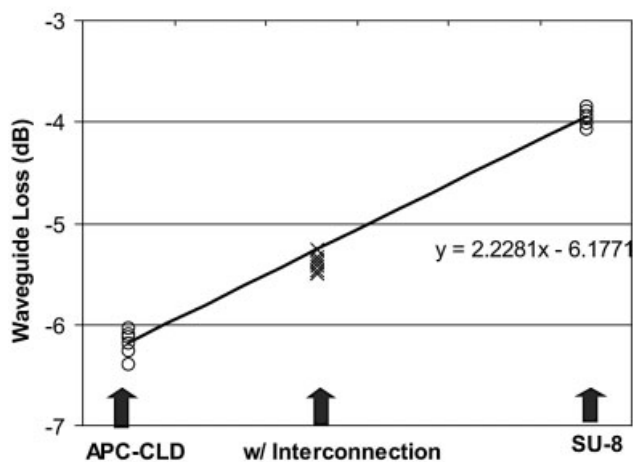


(a)



(b)

Figure 6 Excess-loss test results for waveguide interconnections: (a) inverted ridge-waveguide structure; (b) conventional ridge-waveguide structure

waveguide loss listed here includes the fiber-to-waveguide coupling loss. So the excess losses for the inverted and conventional structure are -0.10 ± 0.15 dB and -0.12 ± 0.15 dB, respectively.

6. CONCLUSION

In this paper, a low-loss interconnection between an EO polymer and a passive polymer has been designed and demonstrated. The structure is simple and easy to fabricate. The excess loss of the interconnection is small and the measurement is limited by the uncertainties in the test. Based on the data, it is safe to say that the excess loss is lower than 0.3 dB and the average of excess loss is around 0.1 dB. This structure has good tolerance to the change of geometric parameters and material properties. It is very suitable for applications in integrated optics, such as PLCs.

REFERENCES

1. M. Oh, H. Zhang, C. Zhang, H. Erlig, Y. Chang, B. Tsap, D. Chang, A. Szep, W.H. Steier, H.R. Fetterman, and L.R. Dalton, Recent advances in electrooptic polymer modulators incorporating highly nonlinear chromophore, *IEEE J Sel Topics Quantum Electron* 7 (2001), 826–835.

2. D.H. Chang, T. Azfar, S-K. Kim, H.R. Fetterman, C. Zhang, and W.H. Steier, Vertical adiabatic transition between a silica planar waveguide and an electro-optic polymer fabricated with gray-scale lithography, *Optics Lett* 28 (2003), 869–871.
3. Y. Enami, M. Kawazu, A.K.-Y. Jen, G. Meredith, and N. Peyghambarian, Polarization-insensitive transition between sol-gel waveguide and electrooptic polymer and intensity modulation for all-optical networks, *J Lightwave Technol* 21 (2003), 2053–2059.
4. M. Oh, C. Zhang, H-J. Lee, W.H. Steier, and H.R. Fetterman, Low-loss interconnection between electrooptic and passive polymer waveguides with a vertical taper, *IEEE Photon Technol Lett* 14 (2002), 1121–1123.
5. T. Watanabe, M. Amano, M. Hikita, Y. Shuto, and S. Tomaru, Novel 'serial grafted' connection between functional and passive polymer waveguides, *Appl Phys Lett* 65 (1994), 1205–1207.
6. S-K. Kim, H. Zhang, D.H. Chang, C. Zhang, C. Wang, W.H. Steier, and H.R. Fetterman, Electrooptic polymer modulators with an inverted rib waveguide structure, *IEEE Photon Technol Lett* 15 (2003), 218–220.

© 2006 Wiley Periodicals, Inc.

PRINTED BAND-NOTCHED ULTRA-WIDEBAND QUASI-DIPOLE ANTENNA

Saou-Wen Su and Kin-Lu Wong

Department of Electrical Engineering
National Sun Yat-Sen University
Kaohsiung 804, Taiwan

Received 22 August 2005

ABSTRACT: A printed ultra-wideband (UWB, 3.1–10.6 GHz) quasi-dipole antenna with the band-notched characteristic is presented. The antenna mainly comprises two radiating elements: an upper semi-circular disk and a lower semi-circular disk embedded with a pair of narrow slits, whose length is about one quarter-wavelength at the desired notched frequency. Both the upper and lower semi-circular disks are of the same dimensions, thus making the proposed antenna tend to be a dipole structure. With a compact size of 25×25 mm², the proposed antenna showing UWB operation with a notched frequency band at 5 GHz is demonstrated. © 2006 Wiley Periodicals, Inc. *Microwave Opt Technol Lett* 48: 418–420, 2006; Published online in Wiley InterScience (www.interscience.wiley.com). DOI 10.1002/mop.21368

Key words: antennas; printed dipole antennas; ultra-wideband (UWB) antennas; band-notched UWB antennas

1. INTRODUCTION

Mainly to avoid the possible interference between ultra-wideband (UWB) systems and existing wireless local area network (WLAN) systems, the band-notching technique has been applied recently to various UWB planar antennas of the frequency band of 3.1–10.6 GHz [1]. These related band-notched planar antennas include planar metal-plate monopole antennas [2, 3], printed monopole antennas [4–6], printed slot antennas [7–9], and so on. It is noted that, among these UWB planar antennas, band-notched operation can be obtained either by loading a proper slot (such as a half-wavelength U-shape slot [2, 3, 6, 8] or a quarter-wavelength V-shape slot [4, 7]) or by inserting proper slits (such as a pair of narrow slits [5, 9]) in the antenna. However, for the band-notched UWB planar antennas reported in the literature, the slot or the slits are generally embedded in the antenna's main radiating element. Seldom is the band-notching achieved by cutting the slot or the slits in the antenna's ground plane, especially for the case of printed monopole antennas.

In this paper, we present a novel band-notched UWB quasi-dipole antenna. The band-notching is achieved by embedding a pair of narrow slits in the antenna's ground plane, with the length of the slits chosen to be a quarter-wavelength of the desired notched frequency. In addition, the antenna is printed on a dielectric substrate, with the ground plane parallel to the antenna's monopole element (see Fig. 1). The monopole element and the ground plane are further selected to be of the same size, which makes it possible to achieve a dipolelike radiation characteristic. A design example of the proposed antenna with a notched frequency band for rejecting the existing 5-GHz WLAN bands of 5.2 GHz (5150–5350 MHz) and 5.8 GHz (5725–5825 MHz) are implemented and studied.

2. ANTENNA DESIGN

Figure 1 shows the proposed printed band-notched UWB quasi-dipole antenna. The antenna is composed mainly of an upper semi-circular disk as the antenna's monopole element and a lower semi-circular disk as the antenna's ground plane. Both the upper and lower semi-circular disks are printed on 0.8-mm-thick FR4 substrate and have the same dimensions (that is, the two disks are of the same diameter D in this design), which makes the proposed antenna tend to be a semi-circular dipole structure [10]. Notice that on the back side of the FR4 substrate is printed the lower semi-circular disk, in which a V-shape notch is cut to serve as the feed gap between the antenna and the ground plane [11]. The monopole element is fed by using a 50 Ω microstrip line of length about one-half the diameter D . In addition, for testing the antenna in the experiment, a 50 Ω SMA connector is used, with its central conductor and outer grounding portion connected to the microstrip line and the ground plane, respectively. With the diameter D chosen to be 25 mm (whose one-quarter perimeter is about 0.2 wavelength of the frequency at 3.1 GHz), the lower-edge frequency of the antenna's impedance bandwidth obtained is less than 3.1 GHz, and good impedance matching across the UWB bandwidth can be achieved.

A pair of narrow slits are embedded at the edge of the lower semi-circular disk (the ground plane) and arranged to be symmetric and parallel to the centerline of the quasi-dipole antenna. The embedded slits have a uniform width of 0.2 mm and a length of 8 mm, and are placed at a distance of 7.5 mm from the microstrip feedline. Note that when the distance increases further, the band-notching characteristic will be degraded. On the other hand, the decreasing distance will in general lead to a wider notched frequency band in the proposed design. By adjusting both the length

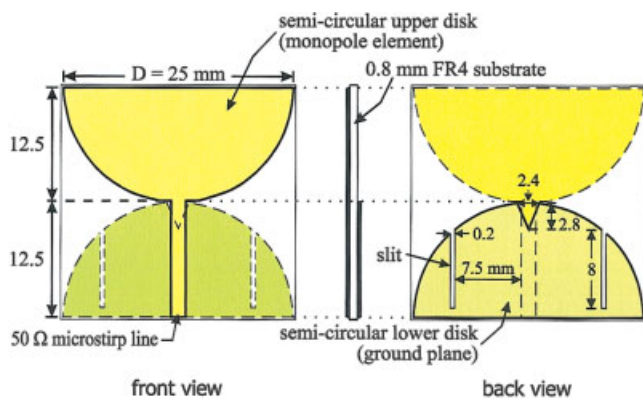


Figure 1 Geometry of the proposed printed band-notched UWB quasi-dipole antenna. [Color figure can be viewed in the online issue, which is available at www.interscience.wiley.com.]

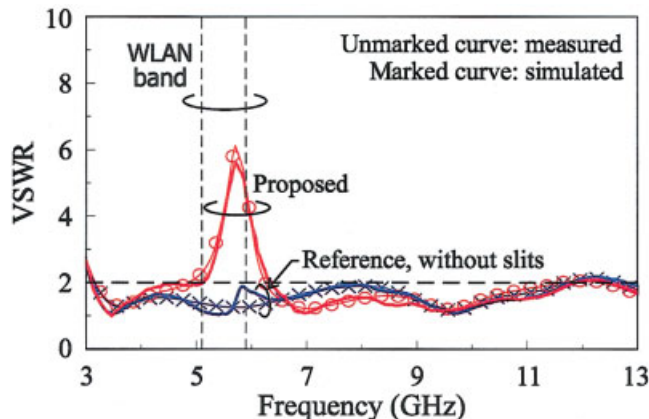


Figure 2 Measured VSWR for the proposed antenna and the reference antenna (the antenna in Fig. 1 without the slits). [Color figure can be viewed in the online issue, which is available at www.interscience.wiley.com.]

of the slits to be about a quarter-wavelength of the desired notched frequency [5], a notched frequency band for the proposed UWB quasi-dipole antenna can be achieved. In this case, a destructive interference for the excited surface currents in the antenna will occur, which causes the antenna to be nonresponsive at that frequency. The detailed simulated surface-current distributions in the antenna at the notched frequency are analyzed in section 3.

3. EXPERIMENTAL RESULTS AND DISCUSSION

Figure 2 shows the measured and simulated VSWR for the proposed antenna and the reference antenna (the case without the slits cut in the lower semi-circular disk). Agreement between the measured data and simulated results obtained using the simulation software Ansoft HFSS (High-Frequency Structure Simulator) [12] is observed. It is seen that an UWB bandwidth (defined by 2:1 VSWR) covering 3.1–10.6 GHz is obtained for the reference antenna. For the proposed antenna, a clear band-notched characteristic is achieved in the 5-GHz WLAN band, with the lowest and highest frequencies of the notched band at about 5.1 and 6.2 GHz, respectively.

Figures 3 and 4 plot the measured radiation patterns at 4 and 8 GHz, respectively. It is first seen that dipolelike radiation patterns are obtained, which are the same as those of the reference antenna

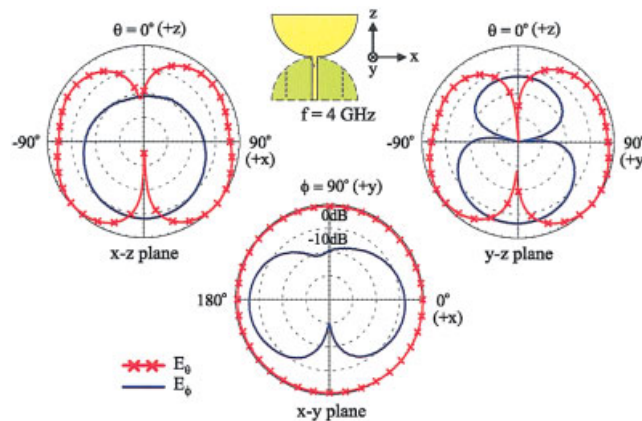


Figure 3 Measured radiation patterns at 4 GHz for the proposed antenna. [Color figure can be viewed in the online issue, which is available at www.interscience.wiley.com.]

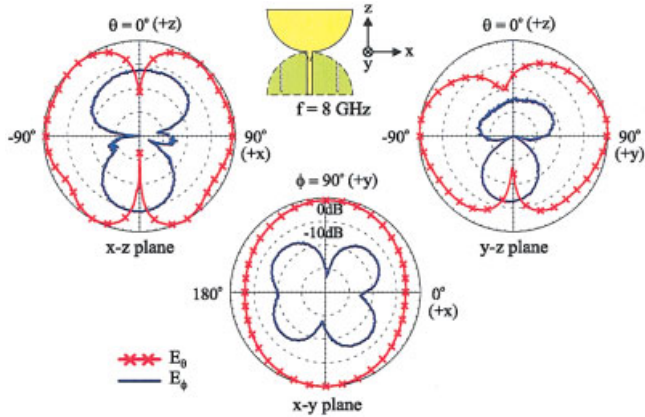


Figure 4 Measured radiation patterns at 8 GHz for the proposed antenna. [Color figure can be viewed in the online issue, which is available at www.interscience.wiley.com.]

(not shown here for brevity). It is also seen that in the azimuthal plane (x - y plane), the antenna tends to have stronger radiation in the $\pm y$ direction than in the $\pm x$ direction, especially for higher operating frequencies. This behavior is generally due to the destructive radiated fields in the $\pm x$ direction caused by the path-length difference of the large antenna width [13]. Also note that special care must be taken to avoid the unwanted radiation from the SMA connector and coaxial line, which can affect the radiation of electrically small UWB antennas to have large ripples as shown in [14], especially for higher operating frequencies in the elevation planes. Figure 5 presents the measured antenna gain for the proposed and reference antennas. The results clearly show a sharp antenna-gain decrease in the notched band.

The simulated (Ansoft HFSS) surface-current distributions in the antenna were also studied. It is observed that, in the lower semi-circular disk, relatively much larger surface current distributions are seen around the slits and the flow of the currents is exactly out of phase on both sides of the slits (see Fig. 6). This characteristic causes the antenna's input impedance to be much larger than 50Ω (about 250Ω at the notched frequency 5.5 GHz), which effectively cuts out the excited surface currents from the microstrip feedline to the upper semi-circular disk (the monopole element), thus making the antenna nonresponsive at that frequency band.

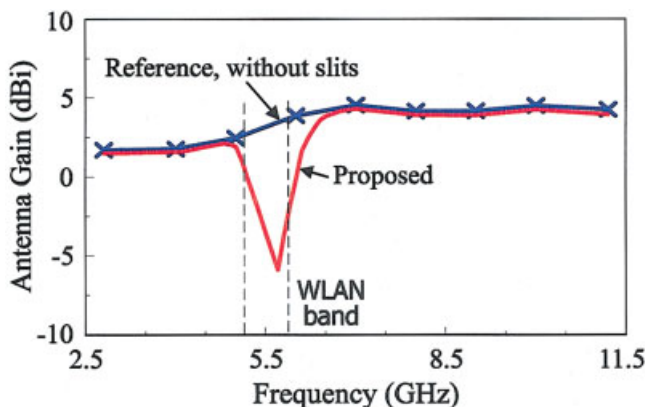


Figure 5 Measured antenna gain for the proposed and reference antennas. [Color figure can be viewed in the online issue, which is available at www.interscience.wiley.com.]

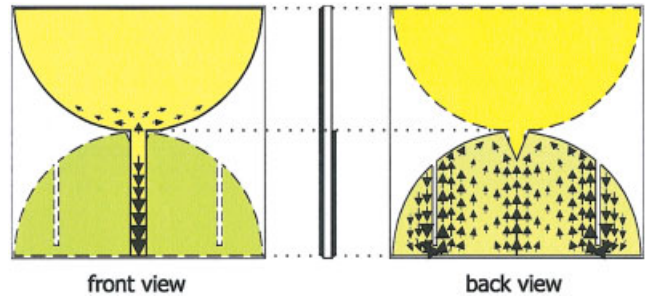


Figure 6 Simulated surface-current distributions at 5.5 GHz for the proposed antenna. [Color figure can be viewed in the online issue, which is available at www.interscience.wiley.com.]

4. CONCLUSION

A microstrip-fed printed UWB quasi-dipole antenna that employs the band-notched technique for rejecting the 5-GHz WLAN bands has been proposed. Band-notching was easily achieved by cutting a pair of narrow slits in the lower semi-circular disk, which functions as the antenna's ground plane. Prototypes of the proposed antenna have been successfully implemented and tested. In addition to the band-notched operation achieved, good dipolelike radiation performances for frequencies out of the rejected band have also been observed.

REFERENCES

1. First Report and Order in the matter of Revision of Part 15 of the Commission's Rules Regarding Ultra-Wideband Transmission Systems, Released by Federal Communications Commission, ET-Docket 98-153, 2002.
2. S.W. Su, K.L. Wong, and C.L. Tang, Band-notched ultra-wideband planar-monopole antenna, *Microwave Opt Technol Lett* 44 (2005), 217–219.
3. K.L. Wong, Y.W. Chi, C.M. Su, and F.S. Chang, Band-notched ultra-wideband circular-disk monopole antenna with an arc-shaped slot, *Microwave Opt Technol Lett* 45 (2005), 188–191.
4. Y. Kim and D.H. Kwon, CPW-fed planar ultra wideband antenna having a frequency band notch function, *Electron Lett* 40 (2004), 403–405.
5. H. Yoon, H. Kim, K. Chang, Y.J. Yoon, and Y.H. Kim, A study on the UWB antenna with band-rejection characteristic, *IEEE Antennas Propagat Soc Int Symp* (2004), Monterey, CA, pp. 1784–1787.
6. K.L. Wong, L.C. Chou, and F.S. Chang, Printed short-circuited wide-band monopole antenna with band-notched operation, *Microwave Opt Technol Lett* 46 (2005), 58–61.
7. Y. Kim and D.H. Kwon, Planar ultra wide band slot antenna with frequency band notch function, *IEEE Antennas Propagat Soc Int Symp*, Monterey, CA, 2004, 1788–1791.
8. S.W. Su, K.L. Wong, and F.S. Chang, Compact printed ultra-wideband slot antenna with a band-notched operation, *Microwave Opt Technol Lett* 45 (2005), 128–130.
9. I.J. Yoon, H. Kim, H.K. Yoon, Y.J. Yoon, and Y.H. Kim, Ultra-wideband tapered slot antenna with band cutoff characteristic, *Electron Lett* 41 (2005), 629–630.
10. H. Schantz, *The art and science of ultrawideband antennas*, Artech House, Boston, 2005, pp. 214–218.
11. C.Y. Huang and W.C. Hsia, Planar elliptical antenna for ultra-wideband communications, *Electron Lett* 41 (2005), 296–297.
12. <http://www.ansoft.com/products/hf/hfss/>, Ansoft Corporation HFSS.
13. K.L. Wong, S.W. Su, and C.L. Tang, Broadband omnidirectional metal-plate monopole antenna, *IEEE Trans Antennas Propagat* 53 (2005), 581–583.
14. J. Liang, C.C. Chiau, X. Chen, and C.G. Parini, Printed circular disc monopole antenna for ultra-wideband applications, *Electron Lett* 40 (2004), 1246–1247.

射频和天线设计培训课程推荐

易迪拓培训(www.edatop.com)由数名来自于研发第一线的资深工程师发起成立,致力并专注于微波、射频、天线设计研发人才的培养;我们于 2006 年整合合并微波 EDA 网(www.mweda.com),现已发展成为国内最大的微波射频和天线设计人才培养基地,成功推出多套微波射频以及天线设计经典培训课程和 ADS、HFSS 等专业软件使用培训课程,广受客户好评;并先后与人民邮电出版社、电子工业出版社合作出版了多本专业图书,帮助数万名工程师提升了专业技术能力。客户遍布中兴通讯、研通高频、埃威航电、国人通信等多家国内知名公司,以及台湾工业技术研究院、永业科技、全一电子等多家台湾地区企业。

易迪拓培训课程列表: <http://www.edatop.com/peixun/rfe/129.html>



射频工程师养成培训课程套装

该套装精选了射频专业基础培训课程、射频仿真设计培训课程和射频电路测量培训课程三个类别共 30 门视频培训课程和 3 本图书教材;旨在引领学员全面学习一个射频工程师需要熟悉、理解和掌握的专业知识和研发设计能力。通过套装的学习,能够让学员完全达到和胜任一个合格的射频工程师的要求...

课程网址: <http://www.edatop.com/peixun/rfe/110.html>

ADS 学习培训课程套装

该套装是迄今国内最全面、最权威的 ADS 培训教程,共包含 10 门 ADS 学习培训课程。课程是由具有多年 ADS 使用经验的微波射频与通信系统设计领域资深专家讲解,并多结合设计实例,由浅入深、详细而又全面地讲解了 ADS 在微波射频电路设计、通信系统设计和电磁仿真设计方面的内容。能让您在最短的时间内学会使用 ADS,迅速提升个人技术能力,把 ADS 真正应用到实际研发工作中去,成为 ADS 设计专家...



课程网址: <http://www.edatop.com/peixun/ads/13.html>



HFSS 学习培训课程套装

该套课程套装包含了本站全部 HFSS 培训课程,是迄今国内最全面、最专业的 HFSS 培训教程套装,可以帮助您从零开始,全面深入学习 HFSS 的各项功能和在多个方面的工程应用。购买套装,更可超值赠送 3 个月免费学习答疑,随时解答您学习过程中遇到的棘手问题,让您的 HFSS 学习更加轻松顺畅...

课程网址: <http://www.edatop.com/peixun/hfss/11.html>

CST 学习培训课程套装

该培训套装由易迪拓培训联合微波 EDA 网共同推出,是最全面、系统、专业的 CST 微波工作室培训课程套装,所有课程都由经验丰富的专家授课,视频教学,可以帮助您从零开始,全面系统地学习 CST 微波工作的各项功能及其在微波射频、天线设计等领域的设计应用。且购买该套装,还可超值赠送 3 个月免费学习答疑...

课程网址: <http://www.edatop.com/peixun/cst/24.html>



HFSS 天线设计培训课程套装

套装包含 6 门视频课程和 1 本图书,课程从基础讲起,内容由浅入深,理论介绍和实际操作讲解相结合,全面系统的讲解了 HFSS 天线设计的全过程。是国内最全面、最专业的 HFSS 天线设计课程,可以帮助您快速学习掌握如何使用 HFSS 设计天线,让天线设计不再难...

课程网址: <http://www.edatop.com/peixun/hfss/122.html>

13.56MHz NFC/RFID 线圈天线设计培训课程套装

套装包含 4 门视频培训课程,培训将 13.56MHz 线圈天线设计原理和仿真设计实践相结合,全面系统地讲解了 13.56MHz 线圈天线的工作原理、设计方法、设计考量以及使用 HFSS 和 CST 仿真分析线圈天线的具体操作,同时还介绍了 13.56MHz 线圈天线匹配电路的设计和调试。通过该套课程的学习,可以帮助您快速学习掌握 13.56MHz 线圈天线及其匹配电路的原理、设计和调试...

详情浏览: <http://www.edatop.com/peixun/antenna/116.html>



我们的课程优势:

- ※ 成立于 2004 年,10 多年丰富的行业经验,
- ※ 一直致力并专注于微波射频和天线设计工程师的培养,更了解该行业对人才的要求
- ※ 经验丰富的一线资深工程师讲授,结合实际工程案例,直观、实用、易学

联系我们:

- ※ 易迪拓培训官网: <http://www.edatop.com>
- ※ 微波 EDA 网: <http://www.mweda.com>
- ※ 官方淘宝店: <http://shop36920890.taobao.com>